Real-time optimization of intermediate temperature for a cascade heat pump via extreme seeking

Wenyi Wang[1] Yaoyu Li[1]

[1]Department of Mechanical Engineering, University of Texas at Dallas, Richardson, TX 75080, U.S.A.
{Wenyi.Wang1, yaoyu.li}@utdallas.edu

Abstract

Improving the energy efficiency of air-source heat pump (ASHP) has been a critical issue for heating operation in cold climates. The cascade heat pump system has been developed as a more advantageous solution over the single-stage heat pump. However, the increased complexity of cascade heat pump systems has presented great challenge for online optimization for the energy efficiency, as model based control/optimization methods incur costly modeling and calibration under different operation and equipment conditions. We propose to use the extremum seeking control as a model-free real-time optimization strategy for efficient operation of cascaded heat pump. The intermediate temperature setpoint is used as the manipulated input for maximizing the system efficiency while satisfying the heating load demand. A Modelica model of an R134a/410a cascade heat pump is developed, and control simulations are conducted for validating the system performance under different ambient conditions.

Keywords: Cascade heat pump, intermediate temperature, extremum seeking control, real-time optimization, Modelica.

1 Introduction

Heat pump has been a mature technology for providing the space or water heating in building operation and industrial processes. However, the performance of the single-stage heat pump can be significantly limited under cold climate operation, which is manifested by decrease in heating capacity and coefficient of performance (COP) as well as increase in discharge temperature. To deal with such challenge, various techniques have been developed to improve the performance of heat pump by enabling higher temperate lift and wider range of ambient temperature, e.g. vapor injections and cascade configuration (Bertsch and Groll 2008; Park et al. 2015; Arpagaus et al. 2016).

In particular, the cascade heat pump can be a viable solution to the limitation of single-stage heat pump (Bansal and Jain 2007). Compared to the single–stage refrigeration cycle, the cascade cycle has a smaller compression ratio for each cycle and exhibits a better compression efficiency (Dopazo et al. 2009; Wang et al. 2009). Then, for the operation of the heat pump system thus implemented, a significantly higher pressure ratio can be achieve even under a low ambient temperature, i.e. resulting in large gap between the condensing pressure and the evaporating pressure.

There have been intensive efforts on optimizing the design and operation of cascade system (Jung et al. 2013; Park et al. 2013; Jung et al. 2014). Kim et al. (2014) conduct experimental and numerical studies on an air-to-water cascade heat pump with R134a/R410A, aiming to find the optimal charge amount. Chae et al. (2015) evaluate the impact of high-temperature cycle refrigerant charge on the performance of a cascade heat pump. Kim et al. (2014) experimentally study the effect of water temperature lift (i.e. the increase of condenser outlet water temperature from the inlet) on the performance of a cascade heat pump with R134a/R410A as the refrigerant. Ma et al. (2018) propose a study for a high-temperature cascade heat pump, using a near-zeotropic mixture BY-3 and R245fa as the working fluids in the low-temperature and high-temperature cycles, respectively. Experimental results show that the cascade heat pump system could reach water outlet temperature of 142°C and the maximum lift of water temperature could reach 100°C. The pressure ratio in the high and low-temperature cycle was 3.4 and 3.9, respectively, with the system COP of 1.72.

Among all the operational parameters for the cascade system, the intermediate temperature, which is the evaporating temperature of a high temperature cycle or the condensing temperature of a low temperature cycle, is deemed the most important. It has direct impact on the compression ratio and compressor isentropic efficiency of each cycle, and thus the COP of the whole system. Therefore, optimizing the intermediate temperature has been a primary focus for the cascade refrigeration or heat pump systems (Lee et al. 2006; Wang et al. 2009; Bhattacharyya 2008; Dopazo et al. 2009). Park et al. (2013) develop a thermodynamic model of a cascade heat pump water heater with R134a and R410A in order to obtain the optimal intermediate temperature. Their numerical analysis was later verified experimentally by Kim et al. (2013).

The existing work on experimental and numerical research has resulted a number of correlations for the optimal intermediate temperature, as for various system configurations. However, such models and the optimal intermediate temperature thus determined are based on elaborate calibration for specific equipment, ambient and load conditions. For practical operation, due to the diverse combinations of operating conditions and equipment status, the model calibration efforts involved can be cost prohibitive. Therefore, real-time control or optimization strategies with least dependency of model knowledge will be highly beneficial.

In this paper, we propose to use the Extremum Seeking Control (ESC) to optimize the setpoint of intermediate temperature (Li et al. 2010; Mu et al. 2015; Hu et al. 2015). More specifically, the low temperature cycle (LTC) condensing temperature is taken as the manipulated input of ESC, while the total power consumption of the system is the only feedback. As for the inner loop control, the LTC compressor speed is used to regulate the intermediate temperature, and the water outlet temperature is regulated by the high temperature cycle (HTC) compressor speed.

The remainder of this paper is organized as follows. The Modelica based dynamic simulation model of the cascade heat pump system is described in next section. Section 3 reviews the ESC principle and design guidelines. Simulation results are presented in Section 4. Section 5 concludes the paper with future work discussed.

2 Dynamic modeling of a cascade heat pump water heater

A cascade heat pump consists of two independently operated single-stage cycles as shown in Fig. 1. The low temperature cycle (LTC) absorbs the heat through evaporator from the ambient air and then transfers the heat to the high temperature cycle (HTC) through an intermediate heat exchanger which is called the cascade heat exchanger. Then the refrigerant in the HTC evaporates in the cascade heat exchanger and then is compressed before entering the condenser where the refrigerant rejects the heat to the water. The cascade heat exchanger works as a condenser for the LTC and evaporator for the HTC. Compared to a single-stage system, the cascade system has a smaller compression ratio and higher compression efficiency for each stage of compression. In this paper, we adopt the typical combination of R410a-R134a for both cycles. Among the most HFC refrigerants, R134a shows a higher critical temperature that is beneficial for making the high temperature hot water (Bertsch & Groll 2008).

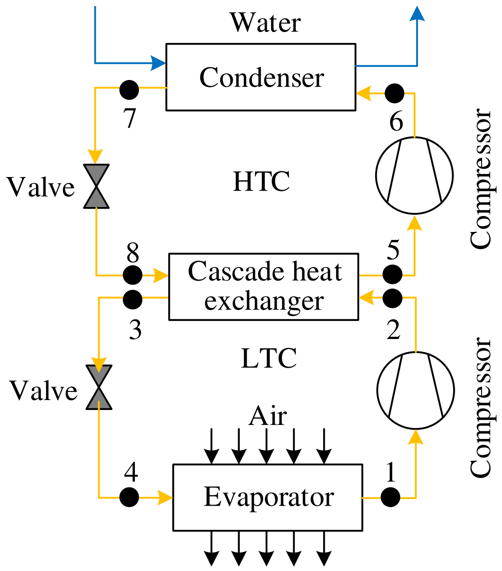

Figure 1. Schematic of a cascade heat pump water heater

Based on these analysis, a Modelica based dynamic simulation model of cascade heat pump is developed using Dymola (Dassault Systems 2017) and TIL Library (TLK-Thermo 2017), as shown in Fig. 2.

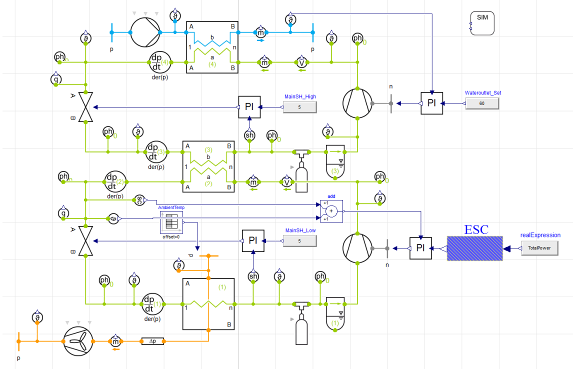

Figure 2. Dymola layout for a cascade heat pump.

In this model, the cascade heat pump system mainly consists of two compressors, three heat exchangers and two-expansion valves. The two compressors for the low and high temperature cycle are both modelled by the scroll compressor module in the TIL Library *TIL.VLEFluidComponents.Compressors.ScrollCompressor* with different displacements. The evaporator for the LTC is modeled with the fin-and-tube cross-flow heat exchanger module *TIL.HeatExchangers.FinAndTube.MoistAirVLEFluid.CrossFlowHX*. The air-side and tube-side convective heat transfer coefficient h_{air} and h_{tube} is calculated by the following equations:

DOI 10.3384/ecp19157251

$$Nu_{air} = 0.31 \Pr^{0.333} \mathrm{Re}^{0.625} \left(\frac{4V_{fin} R_{void}}{D_{tube} A_{fin}} \right)^{0.333} \quad (1)$$

$$h_{tube} = \left(\frac{1.8}{N^{0.8}} \right) \left(\frac{\lambda_{liquid}}{h_{hyd}} * 0.023 \mathrm{Re}^{0.8} \Pr^{0.4} \right) \quad (2)$$

The cascade heat exchanger separates the low temperature refrigerant and high temperature refrigerant, and realizes heat transfer between them. The temperature difference in a cascade heat exchanger is generally considered the most critical parameter that affects the system performance. A large temperature difference in a cascade heat exchanger can lead to degradation of system performance due to the higher irreversibility. To reduce the temperature difference for the cascade heat exchanger, a plate heat exchanger is adopted, modeled by the *TIL.HeatExchangers. Plate.VLEFluidVLEFluid.ParallelFlowHX* module. In the cascade heat exchanger, the low temperature refrigerant evaporates and the high temperature refrigerant condenses. The specific correlation for the evaporating side and condensing side is as follows:

$$h = 0.023 \mathrm{Re}^{0.5} \Pr^{0.4} \left[(1-x)^{0.8} + \frac{3.8x^{0.76}(1-x)0.04}{(p/p_{crit})^{0.38}} \right] \quad (3)$$

$$h = 0.023 \mathrm{Re}^{0.5} \Pr^{0.4} \begin{Bmatrix} (1-x)^{0.01}((1-x)^{1.5} + 1.9x^{0.6}(\frac{\rho_{liquid}}{\rho_{gas}})^{0.35})^{-2.2} \\ +x^{0.01}\left[\left(\frac{\alpha_{gas}}{\alpha_{liquid}} \right) (1+8(1-x)^{0.7}(\frac{\rho_{liquid}}{\rho_{gas}})^{0.67}) \right]^{-2} \end{Bmatrix}^{-0.5} \quad (4)$$

The condenser of the HTC is also modeled by the same plate heat exchanger model. The correlation of refrigerant side is the same as Eq. (4), while the correlation of the waterside follows

$$Nu = 0.122 \Pr * \frac{1}{3} (\frac{\eta_{fluid}}{\eta_{wall}})^{\frac{1}{6}} (\xi * \mathrm{Re}^2 \sin(2\varphi))^{0.374} \quad (5)$$

The orifice valve module *TIL.VLEFluidComponents. Valves.OrificeValve* is used to model the expansion valve, which can calculates the mass flow rate in dependency of the pressure drop using the equation of Bernoulli as follow:

$$m_{flow} = A_{eff} * \sqrt{(p_{input} - p_{output}) * 2\rho_{input}} \quad (6)$$

The evaporator fan is modeled with a simple fan module *TIL.GasComponents.Fans.SimpleFan*, whose operation can be defined with pressure differential or mass flow rate. The water pump is modeled with the *TIL.Liquid Components.Pumps.SimplePump* module, which is an affinity-law based pump model. In this study, the mass flow rate for the air side of the evaporator and the water side of the condenser are both set as constant.

In this study, the two scroll compressor are both controlled by the PI controller, the evaporator fan speed is fixed, so the fan power is constant. The total power is:

$$P_{total} = P_{ucomp} + P_{lcomp} + P_{fan} \quad (7)$$

Then the COP of the cascade water heat pump is the ratio of the heat capacity to the total power:

$$COP = \frac{Q}{P_{total}} \quad (8)$$

The system model is developed based on the ZX-DKFXRS-10II heat pump water heater manufactured by Zhengxu New Energy Equipment Technology Co., Ltd in China. The heat capacity is 58.5 kW under the nominal condition which is defined as: ambient temperature of −12°C dry bulb and −14°C wet bulb, and the water outlet temperature of 85°C. The nominal power consumption is 32.5 kW, the rated volumetric flow rate for the evaporator fan is 30000 m^3/h, and the refrigerant charges for the LTC and HTC are 17 kg and 19 kg respectively. The steady-state characteristics of the simulation model have been validated with the lab testing by the manufacturer, however, the validation data cannot be disclosed by the time of paper preparation.

In this model, the minimal total power corresponds to the maximum COP because of the constant heat capacity maintained throughout the simulated operation. The total power is adopted as the only ESC feedback rather than the COP, because power measurement is relatively simple and cost-effective while determination of COP requires several measurements of thermal and fluidic variables.

3 Extremum seeking control design

ESC deals with the online optimization problem of finding an optimizing input $u_{opt}(t)$ for the generally unknown and/or time-varying cost function $l(t, u)$ (Krstic & Wang 2000; Rotea 2000). The standard gradient based ESC is illustrated in Fig. 3, in which a pair of dither-demodulation signals are used along with high-pass and low-pass filters to extract the gradient information. Closing the loop with integral controller can drive the input to optimality provided that the closed-loop stability is achieved. A typical design guideline for ESC follows Li et al. (2010):

(1) Perform open-loop step test to estimate the input dynamic for the input channel.

(2) The dither frequency should be chosen well within the bandwidth of the input dynamics.

(3) The dither amplitude should be chosen such that the dithered output has sufficient signal-to-noise ratio at the dither frequency.

(4) The dither frequency is generally located in the

pass band of the high-pass filter and in the stopband of the low-pass filter.

(5) The dither-demodulation phase difference integral gain should be chosen to guarantee the asymptotic stability based on some estimate of the input/output dynamics and the Hessian of the static map near the equilibrium.

(6) The integral gain needs to be adjusted to achieve the desirable transient performance under the selected dither signal.

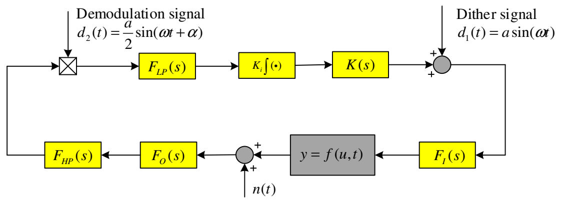

Figure 3. Block diagram of extremum seeking control.

In this study, the ESC controller is used to find the optimal intermediate temperature that can minimize the total power consumption, which is equivalent to maximizing the system COP under fixed heating capacity operation. For the HTC, the water outlet temperature is regulated by the HTC compressor capacity with a proportional-integral (PI) controller, while the superheat of the HTC side of cascade heat exchanger is regulated by the electronic expansion valve (EEV) opening with another PI controller. For the LTC, the evaporator superheat is also regulated by a dedicated EEV, and the intermediate temperature as defined above is regulated by the LTC compressor.

For a cascade heat pump operating in a fixed condition, that means the fixed water inlet and outlet temperature of the condenser and fixed ambient air condition (temperature and relative humidity). A higher low temperature cycle condensing temperature will result in the higher compressor ratio of low temperature cycle, meanwhile it will lead to a lower high temperature cycle compressor ratio because of the fixed heat capacity. The higher compressor ratio means higher power consumption. In the contrary, the lower R410A condenser temperature will results in lower compressor pressure ratio of low temperature cycle and higher-pressure ratio of high temperature cycle. So there exists an optimal R410A condenser temperature which can make a proper pressure ratio for each cycle, and therefore the optimal isentropic efficiency of compressor can be obtained for the each cycle. So in this condition, the total power consumption will be the minimal value. So in a realistic variable ambient air condition, the optimal intermediate temperature changes in real time.

For applying the proposed control strategy in the cascade heat pump to obtain the optimal intermediate temperature therefore the maximal COP and minimal total power, we need to estimate the system input dynamics first in a fixed condition. The hot water inlet temperature is set to be 55°C, and the outlet temperature is regulated to 60°C by the high temperature cycle compressor via a PI controller. The hot water mass flow rater is set to be 0.72 kg/s so that the total heat capacity is the system is fixed at around 15 kW. The ambient air temperature and relative humidity are set to be -7°C and 60% respectively. The air mass flow rate is set to be a constant at 1.85 kg/s. The main loop superheat is fixed at 5°C via a PI controller. For estimating the system dynamics, the simulation is testing under the above condition and the intermediate temperature is regulating from 10°C to 20°C, 20°C to 30°C, 30°C to 40°C, respectively. Based on the simulation results, the normalized response is shown in Fig. 6 and the input dynamics is estimated as

$$\hat{F}_I(s)=\frac{0.021^2}{s^2+2\times0.76\times0.021s+0.021^2} \tag{9}$$

A dither signal with amplitude of 1°C and frequency of 0.005 Hz is then selected. The high-pass and low-pass filters are chosen as

$$F_{HP}(s)=\frac{s^2}{s^2+2\times0.8\times0.0037s+0.0037^2} \tag{10}$$

$$F_{LP}(s)=\frac{0.0032^2}{s^2+2\times0.9\times0.0032s+0.0032^2} \tag{11}$$

4 Simulation Study

In this section, the ESC controller designed in the previous section is evaluated with simulation study using the cascade heat pump system model described earlier.

4.1 Simulation under Fixed Condition

The operation scenario is the same as that described in Section 3. The static map of the total power and COP to the intermediate temperature is shown in Fig. 4, where the intermediate temperature ranges from 10°C to 45°C. The total power achieves the minimal value of 5933.8 Watt at the intermediate temperature of 27.5°C. The COP shows an opposite tendency over the total power profile, achieving the maximum of 2.54 at the same intermediate temperature.

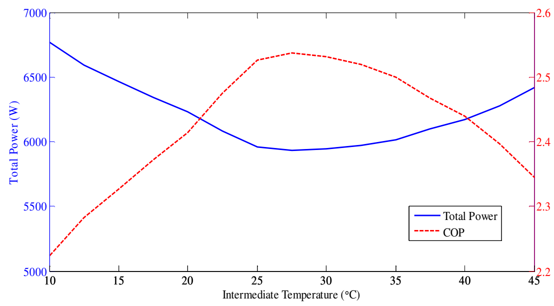

DOI 10.3384/ecp19157251

Figure 4. Static map of total power and COP in terms of intermediate temperature for the cascade heat pump.

The simulation results are shown in Fig. 5 and Fig. 6. The initial HTC compressor speed is fixed at 75 Hz, the LTC compressor speed is fixed at 79 Hz, and the initial intermediate temperature is set to be 20°C. The ESC is turned on at 1 hour and converges after about 3000 seconds. Then the optimal intermediate temperature found by ESC is 29.4°C. Compared to the optimum from the static map in Fig. 3, the steady-state error is about 1.6%. The LTC compressor speed is settled at 90 Hz with the extremum seeking process, and the HTC compressor speed is adjusted to 59 Hz. The total power decreases from 6213.05 W to 5933.77 W, and the COP increases from 2.42 to 2.54, which implies a 4.9% power saving or COP enhancement. It is noteworthy that the water outlet temperature is well stabilized at 60°C with variation less than 0.1°C. The superheats for HTC and LTC are both stabilized at 5°C. This means that the proposed ESC strategy can indeed optimize the system performance by searching for the optimal intermediate temperature, which will make the HTC and LTC operating at their optimal compression ratio. This is achieved by changing the two compressor speeds. The requirements for load demand satisfaction and superheat regulation are all met.

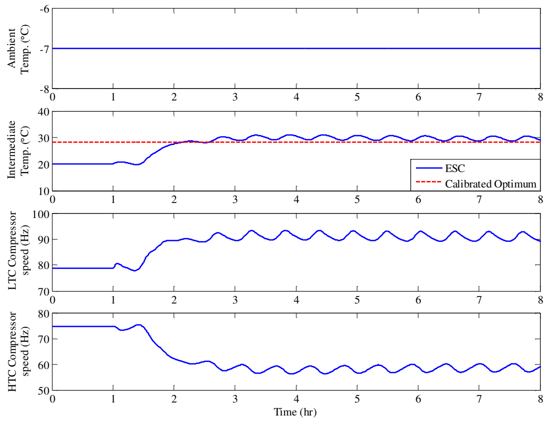

Figure 5. ESC simulation results for the cascade heat pump under fixed ambient temperature.

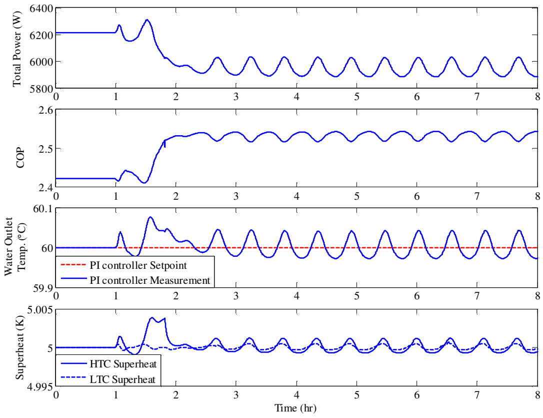

Figure 6. Performance and inner loop regulation for ESC simulation of the cascade heat pump under fixed ambient temperature.

As a further evaluation, the two compressor speeds are set to start at a different combination of initial values. As shown in Fig. 7, the LHC compressor starts at 105 Hz, and for maintaining the heat capacity requirement, the HTC compressor is decreased to 42 Hz. The intermediate temperature is then 42°C. The ESC is also turned on at 1 hour, and converges after about 2000 second. The intermediate temperature found by ESC is 29.6°C, which is consistent with the result from the above case. The HTC and LTC compressor speeds are 90 Hz and 58 Hz, respectively. Similarly, the total power and COP are all as same as the previous result. The performance and inner loop regulation are plotted in Fig. 8.

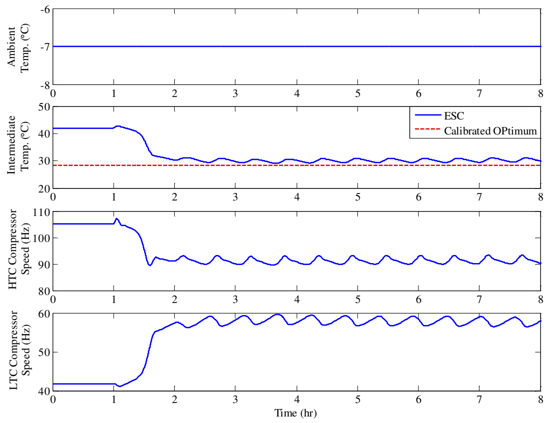

Figure 7. ESC simulation results for the cascade heat pump for second case of fixed ambient temperature.

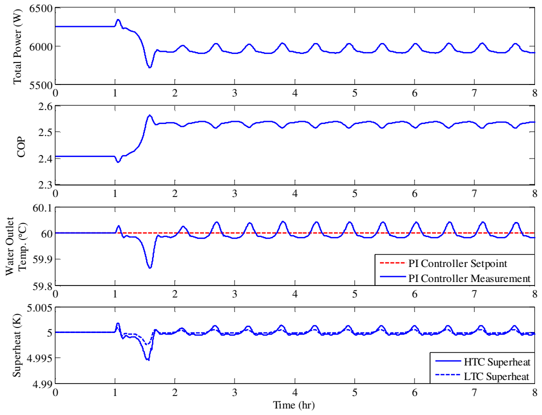

Figure 8. Performance and inner loop regulation for ESC simulation of the cascade heat pump for second case of fixed ambient temperature.

4.2. ESC under variable ambient temperature

The proposed ESC strategy is then evaluated for a staircase ambient temperature profile, as shown in Figs. 9 and 10. The ambient temperature changes from -7°C to -12°C and then -17°C, each change following a 3600-second linear ramp. Fig. 9 shows that the intermediate temperature converges to the respective optimum found the SQP (sequential quadratic programming) procedure offered by the Dymola Optimization Library. The transient time associated with each change of ambient temperature is also reasonable. Fig. 10 shows the energy performance as well as the inner loop regulation, and the results indicate the validity of the ESC search.

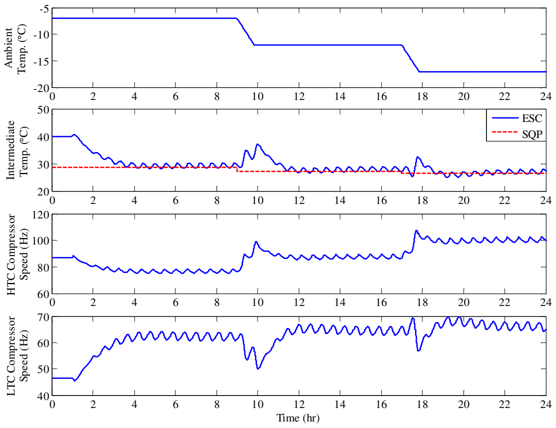

Figure 9. ESC simulation results for the cascade heat pump under staircase profile of ambient temperature.

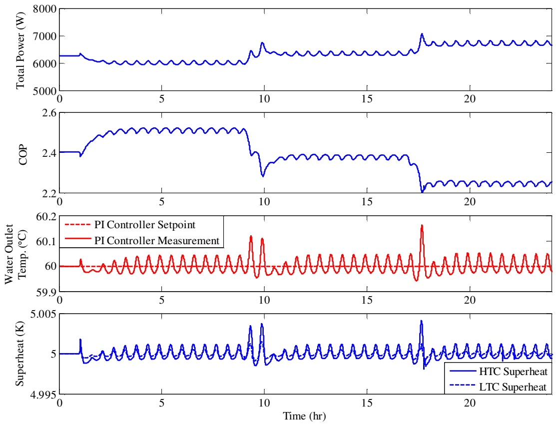

Figure 10. Performance and inner loop regulation for ESC simulation of the cascade heat pump under staircase profile of ambient temperature.

4.3 Simulation under the realistic condition

The ESC strategy is then evaluated with a realistic ambient temperature profile, for which a two-input ESC is designed. Instead of using the intermediate temperature, the compressor speeds for the LTC and HTC are used as the manipulated inputs. From the TMY3 weather data (Buildings.BoundaryConditions. WeatherData.ReaderTMY3), a one-week ambient temperature profile of the O'Hare Airport in Chicago is adopted, which spans January 13 to 20. As shown in the first subplot of Fig. 11, the ambient temperature ranges from −14.4°C to 11.8°C.

As benchmark, the simulation is conducted with the compressor speed fixed at 50 Hz, which is the manufacturer's recommended setting. Then the ESC strategy is simulated. The simulation results for two compressor speeds, intermediate temperature and COP are compared in Fig. 11 for the ESC and benchmark operations. With the ESC strategy, the COP profile is clearly above that under the benchmark operation through the whole-week period being simulated. The largest COP improvement is 15.1% at the maximal ambient temperature of 11.8°C. The smallest COP improvement of 1.1% occurs at the ambient temperature of −12°C, which is exactly the nominal ambient temperature for the equipment design. This is not surprising in that the system operation parameters are optimized for this very condition. The results of heat capacity, total power and water mass flow rate are shown in Fig. 12. The water outlet temperature and superheat are well regulated to their respective setpoints, which justifies the effectiveness of the system operation being simulated.

DOI
10.3384/ecp19157251

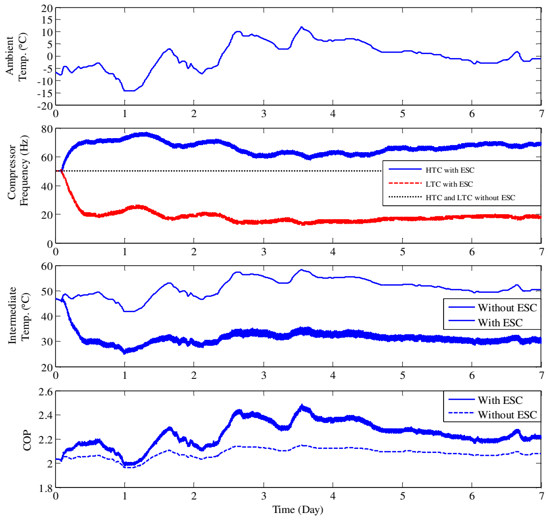

Figure 11 – Trajectories of ambient temperature, compressor speed, intermediate temperature and COP under the realistic condition.

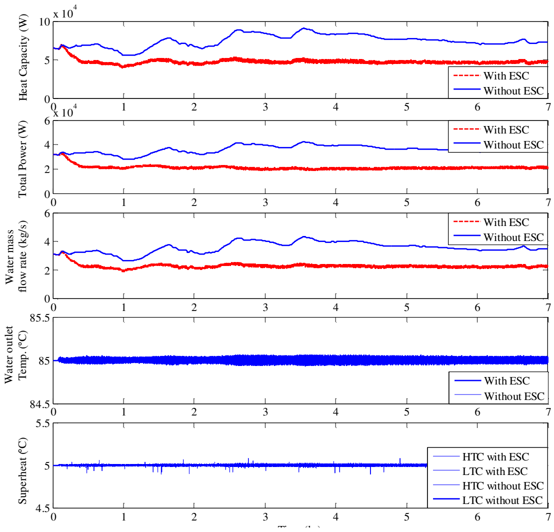

Figure 12. Trajectories of heat capacity, total power, water mass flow rate, water outlet temperature and superheat under the realistic condition.

More simulations are performed under way for different ambient and load conditions.

5 Conclusion

In this paper, we propose an ESC based model free real time optimization method for optimizing the intermediate temperature of cascade heat pump system. A Modelica dynamic simulation model is developed for a cascade heat pump water heating system, using Dymola and TIL Library. Simulations have been performed under fixed, staircase and realistic ambient temperature profiles. Simulation results show that the proposed strategy can converge the operation to pre-calibrated optimum, which promises great benefit for practical operation of the cascade heat pumps systems. Such control strategy requires only power measurement as feedback, which minimizes the sensor requirement. Further work is under way to evaluate the proposed strategy under other operating scenarios.

Acknowledgements

The authors are grateful of TLK-Thermo GmbH for their permission for access to TIL-Suite products, as well as their technical help.

References

C. Arpagaus, F. Bless, J. Schiffmann, and S.S. Bertsch, Multi-temperature heat pumps: A literature review, Int. J. Refrig. 69 (2016) 437-465.

P.K. Bansal, S. Jain, Cascade systems: past, present, and future, ASHRAE Trans. 113 (2007) 245-252.

S. Bhattacharyya, S. Mukhopadhyay, J. Sarkar, CO2-C3H8 cascade refrigeration-heat pump system: heat exchanger inventory optimization and its numerical verification, Int. J. Refrig. 31 (2008) 1207-1213.

S.S. Bertsch, E.A. Groll, Two-stage air-source heat pump for residential heating and cooling applications in northern US climates, Int. J. Refrig. 31 (2008) 1282–1292.

J.H. Chae, J.M. Choi, Evaluation of the impacts of high stage refrigerant charge on cascade heat pump performance, Renewable Energy 79 (2015) 66-71.

Dassault Systems, Dymola: Multi-Engineering Modeling and Simulation based on Modelica and FMI, 2017. < https://www.3ds.com/products-services/catia/products/dymola >.

J.A. Dopazo, J. Fernández-Seara, J. Sieres and F. J. Uhía, Theoretical analysis of a CO2–NH3 cascade refrigeration system for cooling applications at low temperatures, Appl. Therm. Eng. 29 (2009) 1577–1583.

B. Hu, Y. Li, F. Cao, Z. Xing, Extremum seeking control of COP optimization for air-source transcritical CO2 heat pump water heater system, Applied Energy 147 (2015) 361-372.

H.W. Jung, H. Kang, W.J. Yoon, Y. Kim, Performance comparison between a single-stage and a cascade multi-functional heat pump for both air heating and hot water supply, Int. J. Refrig. 36 (2013) 1431–1441.

H.W. Jung, H. Kang, et al., Performance optimization of a cascade multifunctional heat pump in various operation modes, Int. J. Refrig. 42 (2014) 57-68.

D.H. Kim, H.S. Park, M.S. Kim, Optimal temperature between high and low stage cycles for R134a/R410A cascade heat pump based water heater system, Exp. Therm. Fluid Sci. 47 (2013) 172-179.

D.H. Kim, H.S. Park, M.S. Kim, The effect of the refrigerant charge amount on single and cascade cycle heat pump systems, Int. J. Refrig. 40 (2014) 254-268.

D.H. Kim, M.S. Kim, The effect of water temperature lift on the performance of cascade heat pump system, Appl. Therm. Eng. 67 (2014) 273-282.

Krstić, M., Wang, H. H. 2000. "Stability of extremum seeking feedback for general nonlinear dynamic systems." Automatica 36 (4): 595-601.

T. Lee, C. Liu, T. Chen, Thermodynamic analysis of optimal condensing temperature of cascade-condenser in CO2/NH3 cascade refrigeration systems, Int. J. Refrig. 29 (2006) 1100–1108.

P. Li, Y. Li, J.E Seem, Efficient operation of air-side economizer using extremum seeking control, Journal of Dynamic Systems, Measurement, and Control 132 (2010) 031009.

X. Ma, Y. Zhang, X. Li, et al., Experimental study for a high efficiency cascade heat pump water heater system using a new near-zeotropic refrigerant mixture, Appl. Therm. Eng. 138 (2018) 783-794.

B. Mu, Y. Li, J.E Seem, B. Hu, A multivariable Newton-based extremum seeking control for condenser water loop optimization of chilled-water plant, Journal of Dynamic Systems,Measurement, and Control 137 (2015) 111011.

H. Park, D.H. Kim, M.S. Kim, Thermodynamic analysis of optimal intermediate temperatures in R134aeR410A cascade refrigeration systems and its experimental verification, Appl. Therm. Eng. 54 (2013) 319–327.

H. Park, D.H. Kim, M. S. Kim, Performance investigation of a cascade heat pump water heating system with a quasi-steady state analysis, Energy 63 (2013) 283-294.

C. Park, H. Lee, Y. Hwang and R. Radermacher, Recent advances in vapor compression cycle technologies, Int. J. Refrig. 60 (2015) 118-134.

Rotea, M.A., 2000. Analysis of multivariable extremum seeking algorithms. In American Control Conference. Proceedings of the 2000, 433-437, IEEE.

TLK-Thermo GmbH. TIL3.4.2, 2017. <http://www.tlk-thermo.com/index.php>.

B. Wang, H. Wu, J. Li, Z. Xing, Experimental investigation on the performance of NH3/CO2 cascade refrigeration system with twin-screw compressor, Int. J. Refrig. 32 (2009) 1358–1365.

DOI 10.3384/ecp19157251